ACS APPLIED MATERIALS & INTERFACES

Research Article

www.acsami.org

Influence of Substrate Wettability on the Morphology of Thin Polymer Films Spin-Coated on Topographically Patterned Substrates

Sudeshna Roy, Khalid Jamal Ansari, Surendra Sasi Kumar Jampa, Pavanaphani Vutukuri, and Rabibrata Mukherjee*

Department of Chemical Engineering, Indian Institute of Technology Kharagpur, West Bengal, 721 302, India

S *Supporting Information*

ABSTRACT: We show that the morphology of a thin polymer film spin coated directly on to a topographically patterned substrate is strongly influenced by the wettability of the substrate, in addition to other well-known parameters such as concentration of the polymer solution (c_n), spin speed (RPM), and spin duration. Similar to spin coating on a flat surface,[1,2] on a topographically patterned substrate as well, a continuous film forms only above a critical polymer solution concentration (c_t*), for a specific RPM and dispensed drop volume. It is believed that for $c_n > c_t$*, the resulting continuous film on a topographically patterned substrate has an undulating top surface, where the surface undulations are in phase with the underlying substrate patterns.[3] On the basis of experiments involving spin coating of polymer thin films on topographically patterned grating substrates, we show that the surface undulations on the film are in phase with the substrate patterns only when the substrate is completely wetted (CW) by the solvent. In contrast, when the substrate is partially wetted (PW) by the solvent, then the undulations are 180° out of phase with respect to the substrate patterns. We further show that for $c_n < c_t$*, a variety of ordered and disordered structures, like array of aligned droplets, isolated strips of polymers, etc., result on both CW and PW substrates, depending on c_n.

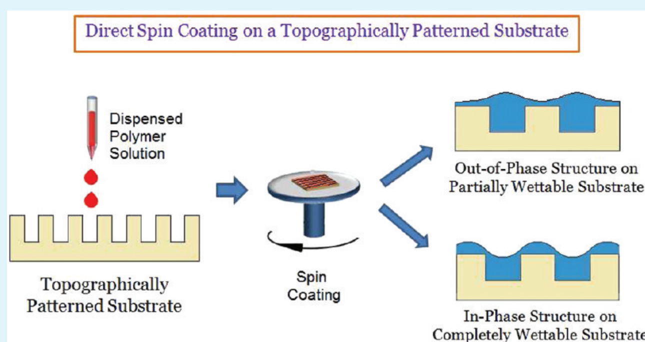

KEYWORDS: *spin coating, out of phase structures, patterned substrates, substrate wettability, meso patterns*

INTRODUCTION

Defect-free thin polymer films and coatings with uniform thickness and covering large areas find important applications as coatings of various types (optical, dielectric, thermal barrier, resist layer in lithography, etc.), lubricants, adhesives, optoelectronic devices, paints, composites, biomembranes, etc.[4−9] It is possible to obtain smooth, uniform films having thickness as low as ∼5 nm on a defect-free, flat substrate by spin coating, with an appropriate choice of solvent, concentration (c_n), and volume of the dispensed polymer solution, spin speed (RPM), and spin duration.[1,2,10−30] Although spin coating in most cases leads to a continuous and smooth film, some specific conditions like very low c_n, extreme nonwettability of the substrate, very high RPM, extremely rapid evaporation of solvent etc., in isolation or in any number of combinations, may hinder the deposition of a continuous film and result in discontinuous, isolated patches of polymer.[1,2,23−28] Stange et al. have shown that spin coating can produce a continuous film only above a critical solution concentration on a flat surface (c_t), and for $c_n < c_t$, either a well-defined network of ribbons or isolated clusters of polymer results.[1] c_t also exhibits rather strong dependence with RPM.[1,18−21,26] Strawhecker et al. suggest that a film rich in rapidly evaporating solvent does not get the necessary time to level the surface undulations caused by Marangoni instabilities and therefore a discontinuous film is likely to result. In contrast, such instabilities are suppressed in favor of a smooth film when the solvent evaporation rate is slow.[26] Weiss and co-workers have shown that the choice of solvent influences the film morphology in spin coating, as they observe the formation of an array of nearly equal sized polymer droplets when a sulfonated polystyrene ionomer is coated on a silica substrate from a 9:1 (v/v) THF/Methanol solution.[27,28] In contrast, a continuous film results when the same polymer is coated from toluene under identical coating conditions.[27,28] Thus, the precise mechanism of film deposition in spin coating is rather complex,[13,14] as three effects independently influence the film formation. These are: (1) centripetal force induced by the high speed rotation; (2) rapid evaporation of the solvent; and (3) wettability of the substrate by the polymer solution, more importantly the solvent, as a very dilute solution is generally used for spin coating. Rotation induced centripetal forces aids in the spreading of the dispensed drop.[13] Evaporation of solvent leads to rapid increase in the viscosity of the polymer film (vis-a-vis reduction in the mobility of the polymer molecules), thereby leading to deposition of the film. The

Received: June 22, 2011
Accepted: April 2, 2012
Published: April 2, 2012

 © 2012 American Chemical Society

rapid evaporation of solvent allows the deposition of a film on a nonwettable substrate, though such a film may be thermodynamically unstable.[18−20] The influence of substrate wettability with respect to the solvent is in fact more complex than the other two: depending on whether the substrate is CW or PW, it may aid or oppose the spreading of the dispensed drop. On a PW substrate, while centripetal force favors spreading of the drop, and thereby film deposition, the substrate wettability opposes it. In contrast both the effects aid spreading and the film deposition on a CW substrate. Surprisingly, the precise influence of substrate wettability (vis-a-vis substrate surface energy, γ_s) on the process of spin coating, particularly its influence on film morphology and film integrity, has not been reported in a comprehensive manner in any of the earlier studies.[1,2,10−30] On the basis of spin coating of polystyrene (PS) from toluene, we show here that c_t is different on a PW and a CW substrate under identical coating conditions, the variation of which is attributed to the antagonistic role of substrate wettability on spreading of the dispensed drop depending on the nature of the substrate.

The film coating process becomes more complex when the polymer film is directly spin coated on to a topographically patterned substrate,[3,31−43] as the topographic structures further influence the morphology of the film, in addition to all the usual parameters that influence the film morphology and thickness on a flat surface. Several papers report direct spin coating of an ultrathin polymer film on a topographically structured substrate, though the views on the morphology of the resulting film are contradicting.[31−43] Rockford et al. argue that there is no tendency of the coated polymer film to planarize the surface, which implies that the amplitude of the substrate features and the amplitude of the undulations on the film are comparable.[32] In contrast, Khare et al. report obtaining discontinuous and isolated strips of polymer on a stripe patterned substrate comprising V grooved channels.[40] One of us, in our previous works have highlighted the issue of likely spatial height variation due to direct spin coating on a topographically patterned substrate.[44,45] However, the widely accepted view in this regards is: (1) a film spin coated on a topographically patterned substrate has an undulating top surface comprising ridges and valleys; (2) the undulations on the film surface are in phase with the substrate patterns; (3) the amplitude of these surface undulations on the film are lower than the amplitude of the substrate patterns; and (4) the amplitude of the film surface undulations progressively reduce with increase in the film thickness.[31,33−39] This understanding suggests that for a continuous film on a grating patterned substrate, each valley and raised ridge of the undulating film is located right above a substrate mesa and a substrate stripe respectively, which is shown either in the form of schematic diagrams or superimposed AFM line scans in several published articles.[31,33−39] A similar trend is also expected on substrates with more complex geometry,[41,42] with the possibility of formation of ordered discontinuous structures at low c_n.[43]

In contrary to general perception, we show in this article for the first time that the undulations on the surface of a thin polymer film directly spin-coated on a grating patterned substrate are in phase with the substrate patterns only when the substrate is completely wetted by the solvent. In contrast, the film undulations are 180° out of phase with respect to the topography of the substrate pattern when the substrate is partially wetted by the solvent of the dispensed polymer. We have checked the authenticity of our results by using different substrates with similar wettability and with different polymers. The formation of 180° out of phase structures on a PW substrate is an important, new observation that significantly alters the fundamental understanding of spin coating on a topographically patterned substrate. The finding is thus relevant to various areas of science which involve spin coating on a topographically patterned substrate, some examples of which include multi layer coating and device fabrication in micro electronics,[46] thin films for optical applications,[47] dewetting of a single and multi layer thin film on a patterned substrate,[33−39] block copolymer ordering,[48] etc. We also show that similar to the existence of c_t on a flat substrate, there exists a critical polymer concentration (c_t*) on a topographically patterned substrate as well, only above which a continuous film can be cast. The magnitude of c_t* varies depending on whether the substrate is PW or CW. Further, on both PW and CW substrates, various ordered and disordered morphologies in the discontinuous films are observed when $c_n < c_t$*. We report the gradual transformation in the as coated film morphology with increase in c_n on grating patterned PW and CW substrates, under identical spinning conditions.

■ EXPERIMENTAL DETAILS

For spin coating of Polystyrene (PS), 200 μL of dilute solution of monodispersed PS (MW: 280K, Sigma, UK) was dispensed on the substrates (both flat and patterned) and spun at 2500 rpm for 1 min in a spin coater (Apex Instruments, India). HPLC-grade toluene was used as the solvent for PS. The concentrations used for coating were 0.01, 0.05, 0.1, 0.125, 0.25, 0.5, 0.60, 0.75, 1.0, 1.5, 2.0, and 3.0 wt % by volume. The coated films were air annealed for 1 h only in order to allow any residual solvent to evaporate and subsequently characterized. No high temperature annealing (even at temperatures below the T_g of PS) was performed as we are interested to investigate the as cast morphology of the films. The resultant structures were investigated using an AFM under intermittent contact mode with a Silicon Cantilever (PPP-NCL, Nanosensors Inc. USA). For checking the non material specific, generic morphology of the films, particularly on the patterned substrates, polymethylmethacrylate (PMMA, MW: 350K, Sigma, UK) films were coated (instead of PS) from toluene in some experiments.

Both flat as well as the patterned substrates were made of ~5 μm thick Sylgard 184 (a 2 part cross-linkable Polydimethylsiloxane (PDMS); Dow Corning, USA) films spin coated from its solution in n-hexane (SRL, India) on cleaned single side polished silicon wafers (test grade, Wafer World, USA). The part A to part B ratio was maintained at 10:1 (v/v) for Sylgard 184, which results in perfectly elastic films.[49,53] For making the topographically patterned substrates, the coated Sylgard films were imprinted with patterned metal foils stripped from commercially available Compact Discs (CD-R) immediately after spin coating. Details about using CD foils for patterning can be found elsewhere.[50−52] The flat as well as the imprinted films along with the foils were cured in an air oven at 120 °C for 12 h for the complete cross-linking of Sylgard 184 and to make the imprinted patterns permanent. The cured samples were cooled to room temperature and the CD foils were peeled off manually (for the imprinted samples). The topography of the patterned substrates was investigated with an AFM (Agilent Technologies, USA; Model: 5100).

The rationale of using a Sylgard substrate was to utilize the CD/DVD foils for patterning them and subsequently use them as topographically patterned substrates. As already reported in the literature, such an approach allows fabrication of structures with regular meso scale features spanning over large areas at extremely low cost, without any formal lithography facility.[50−52] However, as toluene is a good solvent for PDMS as well, one might argues that there can be a possibility of limited swelling of the Sylgard 184 substrates during spin coating of the polymer on these substrate, and subsequent morphologies observed might be experimental artifacts, influenced by

Table 1. Details of the Substrates Used

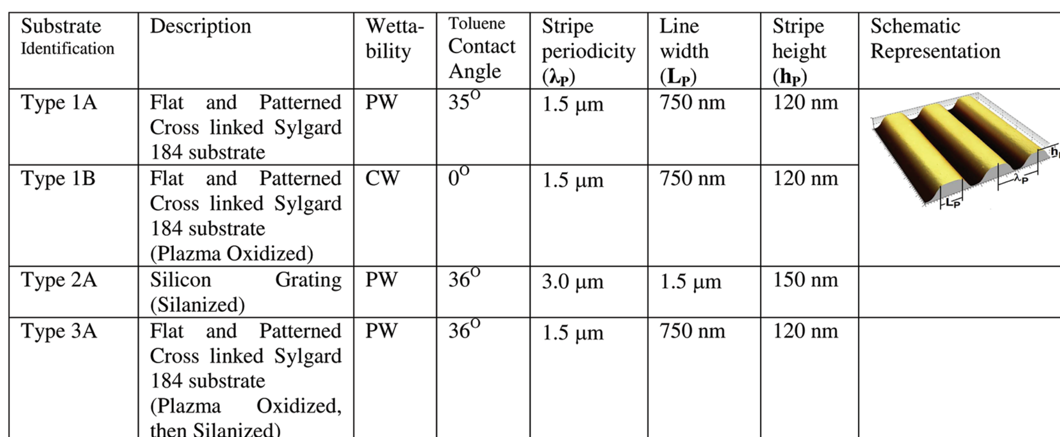

Substrate Identification	Description	Wetta-bility	Toluene Contact Angle	Stripe periodicity (λ_P)	Line width (L_P)	Stripe height (h_P)	Schematic Representation
Type 1A	Flat and Patterned Cross linked Sylgard 184 substrate	PW	35°	1.5 μm	750 nm	120 nm	
Type 1B	Flat and Patterned Cross linked Sylgard 184 substrate (Plazma Oxidized)	CW	0°	1.5 μm	750 nm	120 nm	
Type 2A	Silicon Grating (Silanized)	PW	36°	3.0 μm	1.5 μm	150 nm	
Type 3A	Flat and Patterned Cross linked Sylgard 184 substrate (Plazma Oxidized, then Silanized)	PW	36°	1.5 μm	750 nm	120 nm	

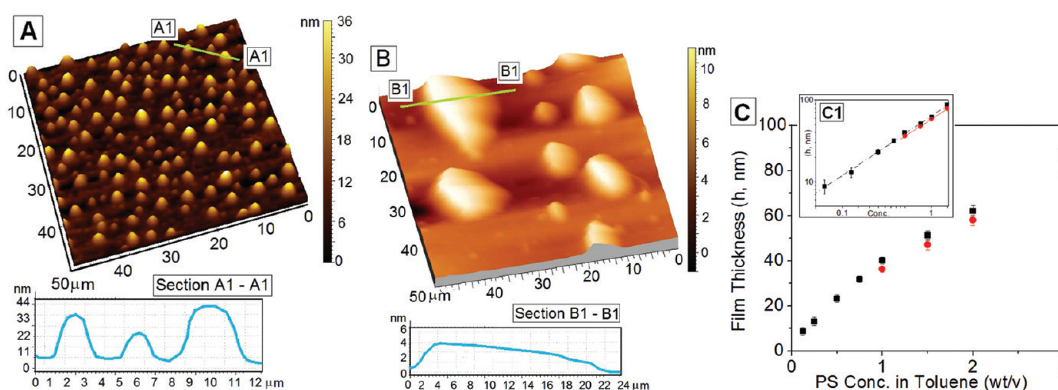

Figure 1. (A) Isolated droplets resulting from spin coating of polymer solution with $c_n \approx 0.50\%$ on a flat type 1A PW substrate. (B) Spread out large droplets resulting from the coating of polymer solution with $c_n \approx 0.005\%$ on a flat, type 1B CW substrate; (C) Variation in h as a function of c_n for continuous films. Red circles indicate PW substrates and black squares CW substrates. Inset shows the same plot on a log−log scale with a best fit to the data.

swelling. On the basis of some additional experiments, described in detail in the Supporting Information, we therefore checked if there is any significant swelling of cross-linked Sylgard 184 substrates during spin coating from toluene solvent and concluded that since the PDMS used as the substrates is fully cross-linked, the dispensed drop volume is very low (~200 μL), and the contact time between the solvent (toluene) and the substrate (cross-linked PDMS) is also very low, there is virtually no swelling of the cross-linked PDMS substrates during spin coating. A recent paper that describes spin coating of a PDMS top layer on a cross-linked PDMS bottom layer also reports that there is no swelling of the substrate due to solvent penetration and validates our observation.[53] Thus, flat and patterned cross-linked PDMS substrates are the ones which have been primarily used in our experiments (type 1A substrates). Cross-linked Sylgard 184 substrates (both flat and patterned) however exhibit partial wettability toward toluene, with an equilibrium contact angle ~35° (measured by contact angle Goniometer, Ramé-hart, Model 290, USA; shown as an inset of figure 2A). To perform experiments on CW substrates with identical geometry, some of the Sylgard 184 substrates were plazma oxidized for 5 min just prior to the coating of the polymer solution (type 1B substrates). Plazma oxidation results in a thin oxide crust film on the PDMS layer on both flat and the patterned Sylgard substrates, making them completely wettable by toluene. (refer to Table 1)

Though we are convinced at this point that there is no effect of substrate swelling even when a cross-linked PDMS substrate is used, we have still used two additional types of substrates, where there is no possibility of swelling at all, to strengthen our observations. For this purpose, we have used some lithographically fabricated silicon gratings as substrates. The silicon gratings, however, exhibit near complete wetting by toluene and therefore cannot be directly used as PW substrates. In order to use them as PW substrates, the gratings were silanized with octadecyl-trichloro-silane (OTS, 95% pure, Aldrich, UK). For silanization, the silicon grids were plazma oxidized for 5 min and then immersed in dilute OTS solution (5 μL of OTS in a 7:3 solution of n-hexadecane and chloroform,) for 1 min. The silanized silicon gratings are referred to as the type 2A substrates. After washing in water and drying, the silanized grids exhibited a toluene contact angle of ~36°, which is roughly same as that observed on patterned cross-linked PDMS substrates.

The plazma oxidized Sylgard substrates themselves were used as the third variety of substrate. The thin stiff oxide layer formed during plazma oxidation itself acts as the diffusion barrier and prevents penetration of any solvent into the Sylgard matrix (refer to the Supporting Information for verification). However, similar to the silicon gratings, the plasma-oxidized substrates are also CW by toluene and therefore, to make them PW, they were also silanized by immersing in an OTS solution. The resulting toluene contact angle was found to be same as that observed in case of silanized silicon grids and cross-linked PDMS substrates. The plazma oxidized and silanized cross-linked PDMS substrates are referred to as type 3A substrates. Both flat and patterned versions of type 3A substrates were used in our experiments. The details about the dimension of the various types of patterned substrates are listed in Table 1.

Film thicknesses of the coated PS films on flat substrates were measured by ellipsometry (EP3). On patterned substrates, there is no simple way to define a film thickness, because of the undulations in film surface, and therefore, an equivalent film thickness on a flat surface under identical coating conditions is some times used.

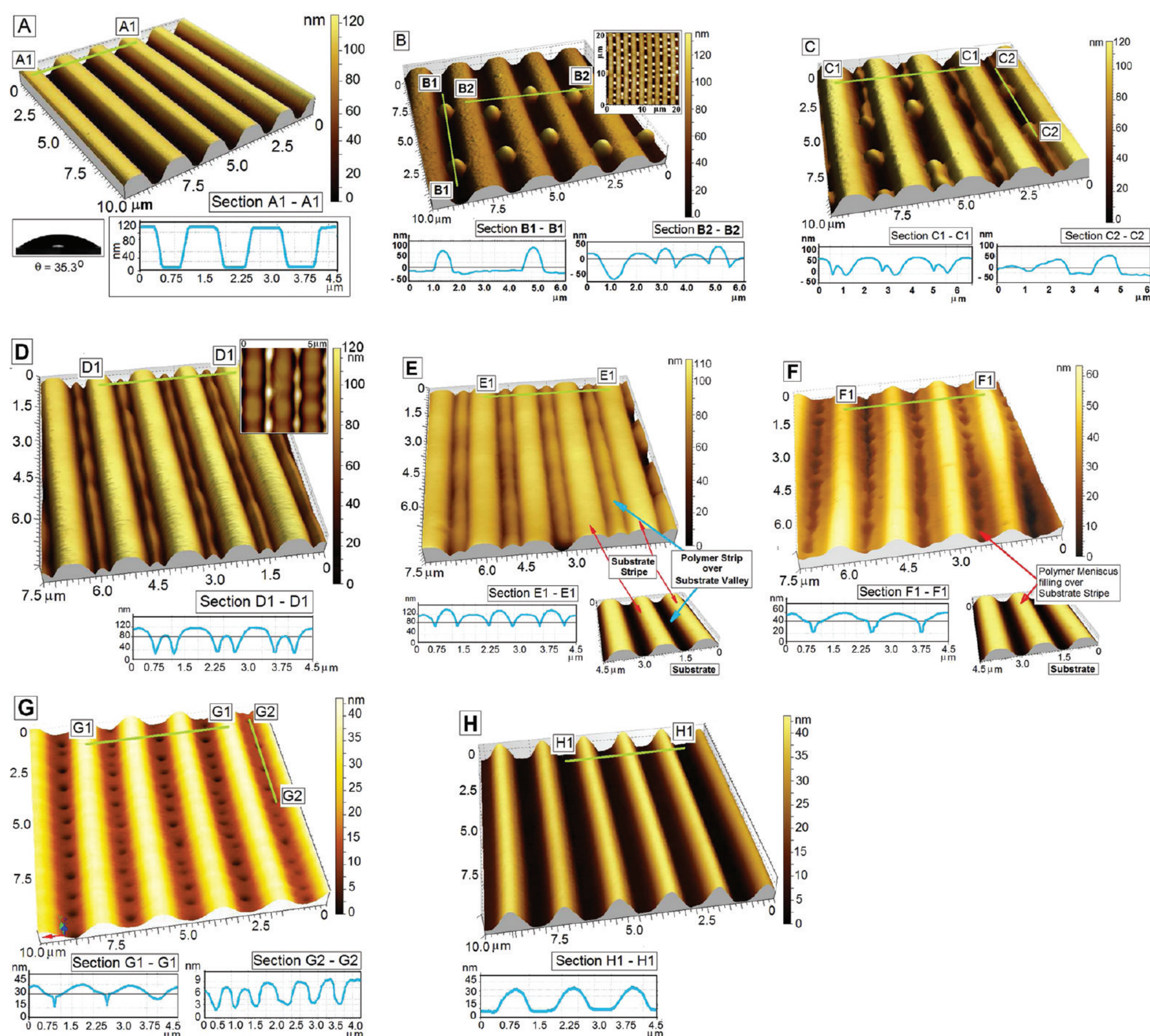

Figure 2. AFM images showing the morphological transition as a function of c_n obtained by direct spin coating of PS solution from toluene on a topographically patterned, type 1A PW substrate. (A) AFM scan of the substrate. Inset shows a contact angle Goniometer image of a drop of toluene dispensed on the substrate, $\theta_E = 35.3°$; (B) Array of droplets for $c_n \approx 0.1\%$. (C) Elongated droplets for $c_n \approx 0.25\%$. (D, E) Thin polymer strips within the channels, for $c_n \approx 0.50$ and 1.25% respectively. The strip in E covers the entire width of the channel, whereas the strip in D is narrower. (F) Signature of advancing meniscus of polymer for $c_n \approx 1.40\%$. (G) For $c_n \approx 1.50\%$, a film morphology where two ridges on the film surface are separated by a valley containing a well ordered array of nearly equal sized holes. (H) A continuous film covering the substrate fully with an undulating top surface for $c_n \approx 1.75\%$. Cross- sectional line scans are shown as insets in each frame. Location of the polymer strips and the advancing meniscus with respect to the substrate is marked in frames E and F, respectively.

RESULTS AND DISCUSSIONS

Spin Coating on a Flat Substrate. Spin coating of a polymer thin film on a flat substrate is rather well investigated,[1,2,10−30] and therefore we have not discussed it in detail here. It has been reported by various researchers that a continuous film results only above c_t, which in turn is a function of the solvent properties (solubility, rate of evaporation), the molecular weight of the polymer, volume of the dispensed drop, spin speed, and duration of spinning (to a lesser extent). We would like to add that in addition to all these parameters, c_t also depends significantly on the substrate wettability. We have obtained a smooth, continuous ≈ 3.5 nm thick PS film on a flat CW type1B substrate for c_n = 0.05%. In contrast, a smooth continuous film on a flat PW substrate (both type 1A and 3A) is obtained only at a relatively high concentration of c_n = 0.75%, with the corresponding film thickness (h) ≈ 28 nm. For all values of c_n < 0.75%, discontinuous films comprising nearly equal sized polymer droplets (Figure 1A) is obtained on a PW substrate. This clearly shows that c_t is strongly influenced by the wettability of the substrate by the solvent. Additional experiments with intermediate c_n shows that c_t lies in the range of $c_n \approx$ 0.60−0.75% on a PW substrate (both for types 1A and 3A), in contrast to value of c_t lying between $c_n \approx$ 0.01 and 0.05% on a CW substrate. The ranges for c_t were found to be nearly the same for PMMA films as well.

At this point, let us focus on the sequence of events or the mechanism that leads to the formation of discontinuous films at low c_n, on a PW substrate. With progress of coating, the solution film becomes thinner because of evaporation and becomes prone to spontaneous rupture, as the substrate does not prefer to remain covered with a layer of the film, which is evident from a negative of spreading coefficient ($S_{SL} = \gamma_s - (\gamma_L + \gamma_{sL})$, $\gamma_s < \gamma_L$ for a PW substrate, γ_{sL} is typically in the range of

dx.doi.org/10.1021/am300201a | ACS Appl. Mater. Interfaces 2012, 4, 1887−1896

1−5 mJ/m^2 and is lower than both γ_s and γ_L).[54] It can be argued (though we could not quantify it) that there is a critical thickness of the solvent rich polymer film (t_s) below which it tends to spontaneously rupture. At lower values of c_n, the thickness of this solution layer becomes thinner than t_s at the later stages of the coating process and consequently the film ruptures and subsequently dewets, forming isolated droplets.[43] In contrast, at higher c_n, presence of higher amount of polymer does not allow the thickness of the solution film to reduce below t_s, during any stages of coating thereby resulting in a continuous film. The argument however does not explain the occurrence of a discontinuous film on a CW substrate also at extremely low values of c_n (Figure 1B), as a positive value of spreading coefficient should always favor the formation of a continuous film. We feel, that on CW substrates the rupture observed can be attributed to substrate heterogeneities, which become pronounce as c_n (and consequently h) becomes very low. The stark contrast in the typical morphology of a discontinuous film on a CW substrate (Figure 1A) and a PW substrate (figure 1B) also validates this opinion. However, it may also be possible that although oxidized PDMS is fully wettable by toluene, it may become partially wettable by concentrated PS solution in the final stages of film thinning because of a higher surface tension of polymer/solution (Could not be verified). This might also lead to rupture in the PS film if the concentration is very low and might explain the formation of droplets (also obtained on a patterned substrate in Figure 5B, discussed later) on CW substrates. The isolated polymer patches in Figure 1B are large, unequal in size and rather random, making very low contact angle with the substrate (~3°), indicating a preferential wetting of the substrate by the polymer. In contrast, the droplets in Figure 1A exhibit much higher contact angle (~22°) with the substrate due its partially wettable nature of it. Further, the type of morphology shown in Figure 1A is very similar to that observed in spontaneous dewetting of thin polymer films,[45,55−57] which is obtained after heating an intact film beyond the T_g of the polymer.[55−57] However, in the present case, the dewetting occurs at room temperature, during the spin coating process itself.

The plot in Figure 1C shows the variation of h on both CW (type 1B) and PW (types 1A and 3A) substrates, as a function of c_n. The role of substrate wettability on spin coating can be clearly noted from the figure: a) a continuous film forms at a much higher c_n vis−a−vis the minimum achievable h is much higher on a PW substrate; and b) for same c_n, h is always slightly (~2−3 nm) higher on a CW substrate. From the plot, the variation of h as a function of c_n appears to be linear. However, a best fit to the data on a log−log plot (shown in inset C1) reveals that h bears a non linear functionality with c_n ($h \approx c_n^{n_1}$), where the best fit exponent $n_1 \approx 0.724 \pm 0.027$ and 0.701 ± 0.039, respectively, for CW and PW substrates. In the absence of a detailed theoretical formulation, it is difficult to quantify the exact significance of the numerical value of n_1, which is ~0.75 regardless of the substrate type. However, qualitatively, we feel that near identical values of n_1 on both types of substrates indicate a rather weak influence of substrate wettability on h as compared to the other dominant parameters like RPM and rate of evaporation of solvent.

Spin Coating on a Stripe Patterned Substrate. Similar to our observation on a flat substrate, on a topographically patterned substrate also we found that a continuous film is possible only above a critical polymer concentration, c_t*. The suffix * is used to distinguish the critical concentration on a patterned substrate from c_t on a flat substrate. It is seen that c_t* is higher on a patterned PW substrate than on a patterned CW substrate. It is further observed that both on a PW and a CW substrate, c_t* > c_t, which implies that the presence of the topographic features on the substrate impose additional resistance toward the formation of a continuous film. Below c_t*, a variety of ordered and disordered patterns forms, which is discussed in the subsequent section.

Figure 2 shows the variety of distinct morphologies obtained when PS solutions with different c_n are directly spin-coated on a stripe patterned cross-linked PDMS substrate (PW, type 1A). Figure 2A shows the AFM scan of the substrate, with the inset showing the toluene contact angle on the substrate. For a low value of c_n = 0.1%, spin coating results in a well-ordered array of nearly equal sized polymer droplets aligned along the channels, as shown in Figure 2B. The inset to the figure shows ordering over a fairly wide area. For c_n in the range of 0.15−0.35%, the morphology gradually changes to elongated and then interconnected droplets, as can be seen in Figure 2C. For c_n in the range of 0.5−1.25%, spin coating results in isolated strips of polymer confined within each channel, as shown in Figure 2D, E. It can also be seen that with an increase in c_n, the width and height of the stripes confined within the channels gradually increases. For example, when c_n = 0.5%, the width and height of the polymer stripes are ~480 ± 12 nm and ~53 ± 3 nm, respectively (Figure 2D). In contrast, when c_n is increased to ~1.25%, the width and height of the stripes change to ~750 nm and ~115 ± 2 nm (Figure 2E), respectively. In the latter case, the entire channel width is filled by the polymer strip. For an even higher c_n = 1.75%, a continuous film fully covering the substrate is obtained. As expected, the top surface of the film is not smooth and it comprises of alternating ridges and valleys (Figure 2H). The periodicity (λ_P) of the ridges is ~1.5 μm, matching identically with λ_P of the substrate stripes. The amplitude of the undulations on the film surface is ~35 nm, which is substantially lower than the original channel depth of 120 nm on the substrate. The amplitude of the undulations on the film surface is seen to further reduce to ~28 nm for c_n = 2%; to ~19 nm for c_n = 3%, and down to ~9 nm for c_n = 5% (images not shown). Further, the ridges on the film surface are of much lower fidelity as compared to the original substrate stripes.

In addition, for an intermediate polymer concentration of c_n = 1.5%, a unique morphology is observed, where the valley separating the two parallel ridges contain a well ordered array of nearly equal sized holes (Figure 2G). The holes have an average diameter of ~163 ± 7 nm and periodicity in the direction of the stripes of ~740 nm. The overall film morphology is unique as it is distinct from the original pattern of the substrate and exhibits ordering at two distinct length scales. The mechanism leading to the formation of the holes is discussed later, in the context of Figure 4. Figure 2F, which corresponds to $c_n \approx$ 1.40% shows a stage just prior to the formation of holes, where one can see the overflow of polymer from the areas above the substrate valleys on to the areas over the stripes. However, the advancing meniscus has not fully joined and holes have not formed. The image sequence clearly shows a gradual transition from a discontinuous film at lower values of c_n < 1.5% to a continuous film for values of c_n > 1.75%. On the basis of our experiments, it can be claimed that in spin coating of PS having a molecular weight of 280K from a solution in toluene (drop volume: 200 μL), c_t* lies between 1.5 and 1.75% on a stripe patterned PW substrate, shown in Figure 2A. It is important to note that c_t* is

significantly higher than c_t, which lies between 0.6 and 0.75% on a featureless, flat PW substrate of the same material. The magnitude of c_t* depends on the molecular weight, the solvent used, and the spin speed also. However, these parametric studies are beyond the scope of this paper. We further add that the morphological transition sequence with increase in c_n is found to be identical on type 2A and type 3A substrates. As the type 1A and type 3A substrates are geometrically identical, near identical morphologies form on both these types of substrates at nearly the same values of c_n. However, as the pattern dimensions of a type 2A substrate is different, the values of c_n at which morphologies similar to that observed on a type 1A/3A substrate are formed is found to be different, though qualitatively the transition sequence remains the same. The details of these set of experimental observation can be found in Figures S2 and S3 in the Supporting Information. A similar transition is also observed for PMMA films on all types (1A, 2A, and 3A) of substrates. The use of different substrates and polymers indeed show that the observations are generic in nature and not material specific.

A detailed look into the morphology of the continuous films in Figure 2H and the substrate in Figure 2A is likely to give an impression that the undulations on the film surface are in phase with the substrate pattern, which means that the ridges on the film surface are above the substrate stripes and the valleys on the film surface are right above the substrate mesas, which indeed is the prevalent notion.[3] Similarly, it also appears that the holes in Figure 2F are located above the substrate mesas. However the relative positioning of the ridges and valleys on the film surface with respect to the underlying substrate pattern can be clearly seen in Figure 3, which is an amplitude contrast

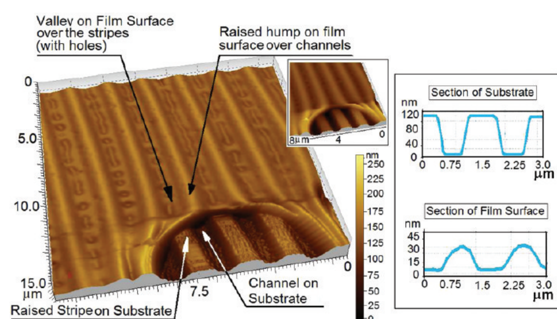

Figure 3. Amplitude contrast image of an area where the film has ruptured, exposing the underlying substrate for a 1.5% PS film spin-coated on a stripe patterned type 1A PW substrate. The exposed area shows that the undulations on the film surface are 180° out of phase with the substrate patterns. It is also seen that the holes on the film surface lie over the substrate stripes. The insets show the amplitudes of the undulations on the film surface and the substrate.

AFM image (topography image is shown as the inset) of a sample where c_n = 1.5%. Similar to that shown in Figure 2F, this particular sample also has an array of holes between two adjacent ridges. The key noticeable feature of the sample is the existence of a defect in the form of a small circular hole over which the film is ruptured, and therefore the uncoated bottom substrate is exposed. It can be clearly seen that each ridge on the film surface is located above a substrate mesa and each valley on the film surface (in this case, containing the holes) lies above a substrate stripe. Thus, the undulating morphology on the film surface is 180° out of phase with respect to the substrate on a patterned PW type 1A substrate. This is an observation that has never been reported before. Several similar experiments were performed by partially removing the film (either by solvent dissolution or by scratching) for different c_n on all types of PW substrates to check the authenticity of the observation shown in Figure 3, and it was indeed seen that in each case, the undulations on the film surface are 180° out of phase with respect to the substrate stripes. The out of phase structure formation was also observed with PMMA films. Several such images and details about the coatings can be found in Figure S4 in the Supporting Information.

The precise morphology of the patterns at a specific concentration on a patterned substrate is found to significantly depend on the RPM. However, the generic transition of the structures, that is, from droplets to a continuous film, occur at different concentrations with variation of RPM. For example, although we observe a morphology comprising array of isolated threads for $c_n \approx 1.25\%$ at 2000 rpm, an array of isolated droplets is observed (similar to that shown in Figure 2B, obtained for $c_n \approx 0.1\%$ for RPM of 2000) is obtained when RPM is 4000 and $c_n \approx 1.25\%$. On the other hand a continuous film (similar to that shown in Figure 2H, for $c_n \approx 1.75\%$ at 2000 rpm) is obtained for $c_n \approx 1.25\%$ itself, at an RPM of 800. Details on this issue can be found in the Supporting Information (item S5).

The illustration in Figure 4 provides an idea about the possible mechanism that leads to the formation of the distinct morphologies on a patterned PW substrate as a function of c_n, as seen in Figure 2. In the early stage of spin coating, a thick (approximately several micrometers; however, we could not measure it) solution (polymer in solvent) layer spreads over the topographically patterned substrate because of the high RPM induced centripetal force. In this stage, the solution layer is much thicker compared to the feature height of the substrate pattern (stage E1, Figure 4). With time, the thickness of the solution layer drastically reduces because of rapid evaporation of the solvent. This leads to reduction of the thickness of the solution layer, which now becomes comparable with the substrate feature height. Concurrently, at this stage the thickness of the solution layer exhibits significant spatial variation: its thickness is lower over the substrate stripes as compared to over the substrate mesas, where it is still thicker (E2, figure 4). At this stage, the solution film breaks over the substrate stripes due to partial wettability of the substrate. Subsequently, the ruptured layer retracts to areas above the substrate mesas. This eventually results in the so-called "bread loaf" morphology (E3, Figure 4), as all the remnant solution accumulates within the channels. At low polymer concentrations, no polymer gets deposited on top of the substrate stripes during the retraction of the solution layer and all the polymer present in the solution gets accumulated over the substrate mesas. This is the key reason for obtaining a discontinuous film at lower c_n. Once the solution film gets localized over the substrate mesas, further evaporation of solvent eventually results in isolated polymer strips within each substrate mesa (A and B, Figure 4). In all cases (A–C, Figure 4), a convex meniscus within the substrate channel is attributed to the partial wettability of the substrate. The convexity of the meniscus can be clearly seen in various frames of Figure 2.

When c_n is very low, the width of the thin polymer strips formed is narrower than the width of the substrate mesa. Eventually, the strip undergoes Rayleigh instability in the axial direction, disintegrating in to isolated droplets aligned along the substrate channels (A2, Figure 4). This type of morphology is

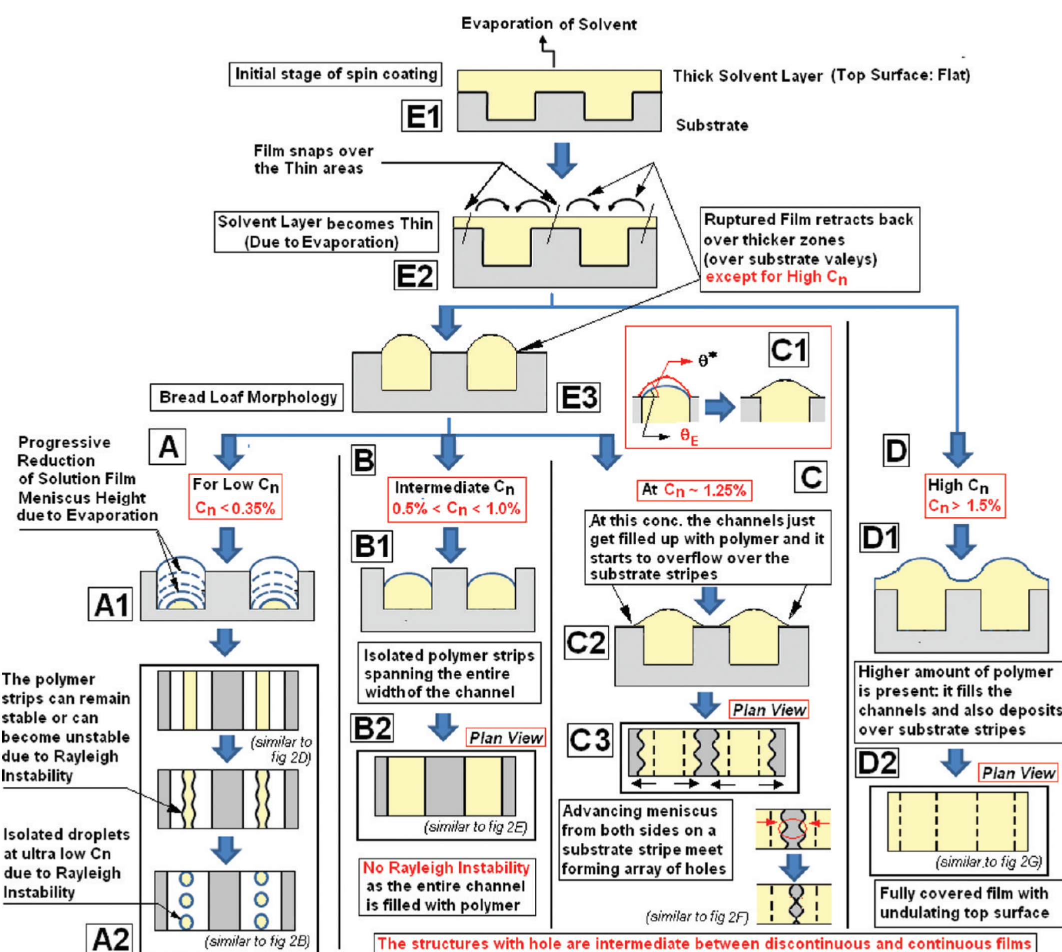

Figure 4. Schematic diagram indicating the possible mechanism leading to formation various ordered and disordered structures by direct spin coating on a patterned PW substrate.

obtained for $c_n \approx 0.10\%$ (Figure 2B). For slightly higher concentrations ($0.15\% < c_n < 0.35\%$), Rayleigh instability sets in, but fails to produce perfectly spherical droplets before the solvents completely evaporate, probably due to a slower dynamics of thicker polymer strips, resulting in elongated and connected droplets (Figure 2C). At slightly higher c_n, the dynamics of the system becomes even more sluggish as the thickness of the polymer strips increases. This in turn results in intact strips, though the width of each strip is narrower than the channel width, as can be seen in Figure 2D. Clear axial undulations due to Rayleigh instability in these intact stripes can be seen in the 2D AFM image shown as the inset to Figure 2D. The long stripes of polymer are thermodynamically unstable but remain intact, as the solvent evaporates before the instability can set in. Once the polymer strips become devoid of solvent their viscosity becomes very high and no further morphological reorganization becomes possible, resulting in kinematically stabilized narrow, undulating strips. With further increase in c_n ($0.5\% < c_n < 1.0\%$), the isolated polymer strips become wider, covering the entire width of each channel, and in the process the Rayleigh instability gets completely suppressed (Figure 2E and inset B2, Figure 4). This results in stable, isolated parallel strips of polymer covering each substrate mesa. The shape of the meniscus is governed by the equilibrium contact angle (θ_E) of the polymer with the substrate material. With increase in c_n, if excess polymer gets deposited over the completely filled up substrate channels, then the in situ contact angle θ^* exceeds θ_E, which immediately triggers an over flow of polymer, resulting in the spreading of the polymer meniscus over the two adjacent substrate stripes, as schematically shown in inset C1, Figure 4. The AFM morphology corresponding to this scenario can be seen in Figure 2F. Actually the overflow marks the transition from a discontinuous film with separate strips of polymer confined within each channel to a continuous film, when the two adjacent over flowing polymer meniscus meet each other over a substrate stripe, forming a continuous film. This morphology is shown in figure 2H. The AFM images in Figure 2F, G show morphologies where two adjacent advancing meniscuses have not joined up fully. In Figure 2F, the two advancing meniscuses have not met at all, leaving a sharp gap between the two and exposing part of the substrate stripe. In contrast, in Figure 2G, the two advancing meniscuses have joined but not fully, due to inadequate amount of polymer present, resulting in the formation of small holes along the line of joining of the two advancing meniscuses, on top of the substrate stripes, which can be seen in Figures 2G and 3. The structure with holes forms for a very narrow range of polymer concentration of ~1.5%. For concentrations slightly higher than $c_n \approx 1.5\%$ a continuous film forms. We feel that although joining of two adjacent advancing meniscuses indeed leads to the formation of a continuous film, for higher concentrations of c_n, there is also direct deposition of polymer on the stripe tops, which joins up with the advancing meniscus, forming a continuous film. This

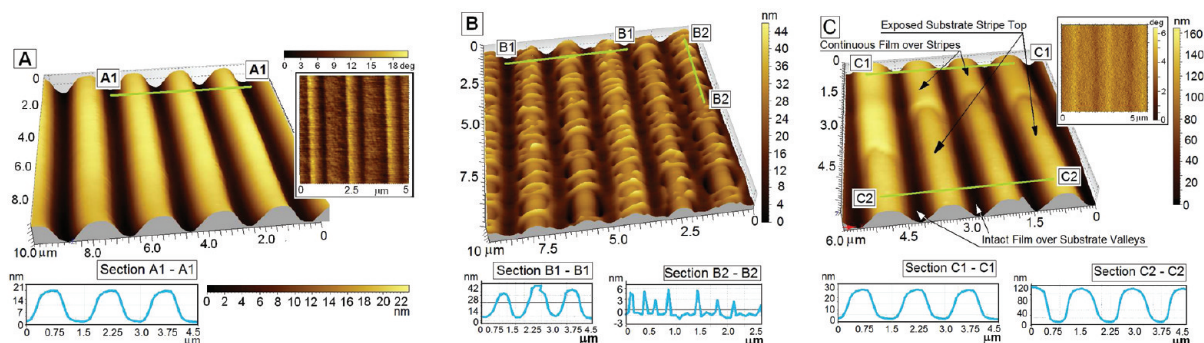

Figure 5. Different morphology of PS films spin coated on patterned CW (type 1B) substrates: (A) Isolated polymer strips with concave meniscus for c_n = 0.25%. The polymer strips and the substrate stripes can be clearly distinguished in the phase contrast image, shown as the inset. (B) Transition from a discontinuous film to a continuous film with formation of polymer bridges over substrate stripes across two polymer strips confined within two adjacent channels, for c_n = 0.45%. (C) A continuous film with undulating top surface for c_n = 0.75% The film in image C is partially damaged, exposing part of the substrate, which confirms that the undulations on the film surface are in phase with the substrate patterns. Insets show cross-sectional line scan in each frame.

mechanism is suggested in scheme D in Figure 4. However, we do not have any direct visual confirmation of this suggested mechanism. As already pointed out, the same morphological transition sequence is observed on all types of patterned PW substrates used in our experiments.

On a patterned CW substrate (type 1B), the morphology of the spin coated film with variation of c_n is drastically different. In contrast to obtaining a continuous film at $c_t^* \approx 1.75\%$ on a PW substrate, a continuous PS film is obtained at a concentration as low as $c_n \approx 0.50\%$ itself. Although the film surface at this concentration is undulated, similar to that observed on PW substrates, it can be clearly seen in Figure 5C (shows partially bare substrate along with the film) that the undulations on the film surface are in phase with the substrate patterns. Further, unlike on PW substrate, on a patterned CW substrate isolated droplet along the stripes are never observed, even at very low c_n, down to 0.01%. However, for $c_n \leq 0.25\%$, discontinuous films in the form of isolated polymer strips in each substrate mesa are obtained (Figure 5A). The morphology of the strips, however, is distinctly different from those obtained on a PW substrate, as the polymer meniscus, because of preferential wetting is concave with in a completely wetted channels, in contrast to a convex meniscus seen on a patterned PW substrate, resulting from partial wetting and retraction of contact line. The formation of isolated polymer strips is confirmed from the phase contrast image shown as the inset to Figure 5A, which shows a significantly higher (~18°) phase lag between the stripes and the substrates, in comparison to a phase difference of only ~6° observed in the phase contrast image of a continuous film on a patterned CW substrate shown as inset to Figure 5C. Figure 5B shows the transition from the discrete, isolated stripes to a continuous film on a type 1B substrate, for intermediate values of $c_n \approx 0.30{-}0.45\%$. However, the formation of the threads can also be attributed to a higher surface energy of the polymer at the later stages of spinning process. The transition on a CW substrate is with the formation of polymer bridges connecting the isolated strips confined within two adjacent substrate mesas. With gradual increase in the polymer concentration, the number of spars of polymer over a substrate stripe bridging the two adjacent strips increase, eventually covering the whole substrate stripe and resulting in a continuous undulating film. Thus the value of $c_t^* \approx 0.50\%$, on a patterned CW substrate, which is far lower than a value of $c_t^* \approx 1.5\%$ on a patterned PW substrate having the same geometry.

■ CONCLUSION

In this paper, we have experimentally shown the influence of substrate wettability on the morphology as well as integrity of a spin coated film, on a flat surface as well as on a topographically patterned substrate. The critical polymer concentration (c_t) at which a continuous film forms on a flat PW substrate is much higher (~0.6%−0.7%) than a value of c_t ~0.01%−0.05% on a CW substrate. In other words, it becomes possible to spin-cast a much thinner film on a CW substrate as compared to a flat PW substrate. The minimum film thicknesses we could achieve were ~3.5 nm and ~28 nm on a flat CW and PW substrate, respectively. For $c_n < c_t$, particularly on PW substrates, an array of isolated droplets are obtained. We further show that even at concentrations where a continuous film is obtained both on a CW and a PW substrate, h on a CW substrate remains slightly higher (2−3 nm higher) than that obtained on a PW substrate, because of the preferential wetting on the former type of substrate.

On a topographically patterned substrate comprising stripes, we show that both for a PW and a CW substrate, a continuous film forms only above a critical concentration (c_t^*) of the dispensed drop. Similar to our observation on a flat substrate, c_t^* is also higher for a PW substrate (~ 1.5%) in comparison to a CW substrate (~0.5%), having identical geometry. Above c_t^*, on both types of substrates, a continuous film with an undulating top surface results. The amplitude of these surface undulations progressively diminishes with increase in c_n, on both the type of substrates. Most importantly, although the undulations are in phase with the substrate patterns on a CW substrate, they are found to be 180° out of phase with respect to the substrate structures on a PW substrate. This is a very significant, new finding, which is reported in this paper for the first time. The 180° out of phase structures form on variety of different substrates that exhibit partial wettability toward toluene, which has been used as the solvent in this study. Limited number of experiments performed with other solvents (Choloroform, MEK etc.) also shows the formation of the out of phase structures on PW substrates, which has also been obtained with polymers other than PS (verified with PMMA, refer to Figure S4 in the Supporting Information for details).

dx.doi.org/10.1021/am300201a | ACS Appl. Mater. Interfaces 2012, 4, 1887−1896

We further show for $c_n < c_t^*$, a variety of ordered and disordered structures like array of droplets, elongated droplets, isolated polymer strips, and undulating film with alternate ridges separated by valleys containing aligned array of nearly equal sized holes etc. form, which suggest that spin coating with a low c_n itself has the potential to develop into a possible meso patterning technique. We have also proposed suitable mechanisms for the formation of the different structures on the PW and CW substrates.

We would like to point out that several other parametric variations like choice of polymer and solvent (studied to a limited extant in this paper), molecular weight of the polymer, spin speed, substrate pattern geometry, etc. are likely to significantly influence the results and detailed investigations on the role of each one of these parameters will surely result in interesting case studies. Finally, we feel that the results reported in this article are significantly new and to some extent alter our basic understanding of spin coating of a thin polymer film on a topographically structured substrate, a problem that is extremely relevant in various technologically important areas like micro electronics, casting various types of coatings, fabrication of planar optical waveguides etc.

■ ASSOCIATED CONTENT

Supporting Information

Additional figures and information (PDF). This material is available free of charge via the Internet at http://pubs.acs.org.

■ AUTHOR INFORMATION

Corresponding Author

*Tel: +91-3222 283912. E-mail: rabibrata@che.iitkgp.ernet.in.

Notes

The authors declare no competing financial interest.

■ ACKNOWLEDGMENTS

The authors acknowledge the support of the Department of Science & Technology (DST), New Delhi, India, for funding the research under its Nano Mission program (SR/NM/NS-63/2010). R.M. acknowledges the IUSSTF – Indo US Centre for Research Excellence on Fabrionics, for funding the Atomic Force Microscope (AFM).

■ REFERENCES

(1) Stange, T. G.; Mathew, R.; Evans, D. F.; Hendrickson, W. A. *Langmuir* **1992**, *8*, 920.

(2) Extrand, C. J. *Langmuir* **1993**, *9*, 475.

(3) Mukherjee, R.; Pangule, R. C.; Sharma, A.; Banerjee, I. *J. Chem. Phys.* **2007**, *127*, 064703.

(4) Garbassi, F.; Morra, M.; Occhiello, E. *Polymer Surfaces: From Physics to Technology*; John Wiley & Sons: New York, 2002.

(5) Singh, J.; Agrawal, K. K. *J. Macromol. Sci.* **1992**, *32*, 521.

(6) Mayer, W. H. *Adv. Mater.* **1998**, *10*, 439.

(7) Friend, R. H.; Gymer, R. W.; Holmes, A. B.; Burroughs, J. H.; Marks, R. N.; Taliani, C.; Bradley, D. D. C.; Dos Santos, D. A.; Breads, J. L.; Logdlund, M. L.; Salaneck, W. R. *Nature* **1999**, *397*, 121.

(8) Kelley, T. W.; Baude, P. F.; Gerlach, C.; Ender, D. E.; Muyres, D.; Haase, M. A.; Vogel, D. E.; Theiss, S. D. *Chem. Mater.* **2004**, *16*, 4413.

(9) Gonuguntla, M.; Sharma, A.; Mukherjee, R.; Subramanian, S. A. *Langmuir* **2006**, *22*, 7066.

(10) Emslie, A. G.; Bonner, F . T.; Peck, C. G. *J. App. Phys.* **1958**, *29*, 858.

(11) Acrivos, A.; Shah, M. G.; Peterson, E. E. *J. Appl. Phys.* **1960**, *31*, 963.

(12) Bornside, D. E.; Macosko, C. W.; Scriven, L. E. *J. Imag. Technol.* **1987**, *13*, 122.

(13) Lawrence, C. J. *Phys. Fluids* **1988**, *31*, 2786.

(14) Bornside, D. E.; Macosko, C. W.; Scriven, L. E. *J. Appl. Phys.* **1989**, *66*, 5185.

(15) Hall, D. B.; Underhill, P.; Torkelson, J. M. *Polym. Eng. Sci.* **1998**, *38*, 2039.

(16) Meyerhofer, D. *J. Appl. Phys.* **1978**, *49*, 3993.

(17) Lai, J. H. *Polym. Eng. Sci.* **1979**, *19*, 1117.

(18) Chen, B. T. *Polym. Eng. Sci.* **1983**, *23*, 399.

(19) Weill, A.; Dechenaux, E. *Polym. Eng. Sci.* **1988**, *28*, 945.

(20) Lawrence, C. J. *Phys. Fluids A* **1990**, *2*, 453.

(21) Spangler, L. L.; Torkelson, J. M.; Royal, J. S. *Polym. Eng. Sci.* **1990**, *30*, 644.

(22) Bornside, D. E.; Macosko, C. W.; Scriven, L. E. *J. Electrochem. Soc.* **1991**, *138*, 317.

(23) Extrand, C. W. *Polym. Eng. Sci.* **1994**, *34*, 390.

(24) Frank, C. W.; Rao, V.; Despotopoulou, M. M.; Pease, R. F. W.; Hinsberg, W. D.; Miller, R. D.; Rabolt, J. F. *Science* **1996**, *273*, 912.

(25) Shapovalov, V.; Zaitsev, V. S; Strzhemechny, Y.; Choudhery, F.; Zhao, W.; Schwarz, S. A.; Ge, S.; Shin, K.; Sokolov, J.; Rafailovich, M. H. *Polym. Int.* **2000**, *49*, 432.

(26) Strawhecker, K. E.; Kumar, S. K.; Douglas, J. F.; Karim, A. *Macromolecules* **2001**, *34*, 4669.

(27) Weiss, R. A.; Zhai, X.; Dobrynin, A. V. *Langmuir* **2008**, *24*, 5218.

(28) Zhai, X.; Weiss, R. A. *Langmuir* **2008**, *24*, 12928.

(29) Perlich, J.; Krstgens, V.; Metwalli, E.; Schulz, L.; Georgii, R.; Muller-Buschbaum, P. *Macromolecules* **2009**, *42*, 337.

(30) Norrman, K.; Ghanbari-Siahkali, A.; Larsen, N. B. *Annu. Rep. Prog. Chem. (Sect. C)* **2005**, *101*, 174.

(31) Li, Z.; Tolan, M.; Hohr, T.; Kharas, D.; Qu, S.; Sokolov, J.; Rafailovich, M. H.; Lorenz, H.; Kotthaus, J. P.; Wang, J.; Sinha, S. K.; Gibaud, A. *Macromolecules* **1998**, *31*, 1915.

(32) Rockford, L.; Liu, Y.; Mansky, P.; Russell, T. P.; Yoon, M.; Mochrie, S. G. J. *Phys. Rev. Lett.* **1999**, *82*, 2602.

(33) Rehse, N.; Wang, C.; Hund, M.; Geoghegan, M.; Magerle, R.; Krausch, G. *Eur. Phys. J. E* **2001**, *4*, 69.

(34) Kargupta, K.; Sharma, A. *Langmuir* **2002**, *18*, 1893.

(35) Zhang, Z.; Wang, Z.; Xing, R.; Han, Y *Polymer* **2003**, *44*, 3737.

(36) Luo, C.; Xing, R.; Zhang, Z.; Fu, J.; Han, Y. *J. Colloid Interface Sci.* **2004**, *269*, 158.

(37) Luan, S.; Cheng, Z.; Xing, R.; Wang, Z.; Yu, X.; Han, Y. *J. Appl. Phys.* **2005**, *97*, 086102.

(38) Geoghegan, M.; Wang, C.; Rehse, N.; Magerle, R.; Krausch, G. *J. Phys.: Condens. Matter* **2005**, *17*, S389.

(39) Bandyopadhyay, D.; Sharma, A.; Rastogi, C. *Langmuir* **2008**, *24*, 14048.

(40) Khare, K.; Brinkmann, M.; Law, B. M.; Gurevich, E. L.; Herminghaus, S.; Seemann, R. *Langmuir* **2007**, *23*, 12138.

(41) Xing, R.; Luo, C.; Wang, Z.; Han, Y. *Polymer* **2007**, *48*, 3574.

(42) Yoon, B.; Acharya, H.; Lee, G.; Kim, H.-C.; Huh, J.; Park, C. *Soft Matter* **2008**, *4*, 1467.

(43) Ferrell, N.; Hansford, D. *Macromol. Rapid Commun.* **2007**, *28*, 966.

(44) Mukherjee, R.; Gonuguntla, M.; Sharma, A. *J. Nanosci. Nanotechnol.* **2007**, *7*, 2069.

(45) Mukherjee, R.; Bandyopadhyay, D.; Sharma, A. *Soft Matter.* **2008**, *4*, 2086.

(46) Kelley, T. W.; Baude, P. F.; Gerlach, C.; Ender, D. E.; Muyres, D.; Haase, M. A.; Vogel, D. E.; Theiss, S. D. *Chem. Mater.* **2004**, *16*, 4413.

(47) Willey, R. R. *Practical Design and Production of Optical Thin Films*, 2nd ed.; Marcel Dekker: New York, 2002.

(48) Lee, G.; Jo, P. S.; Yoon, B.; Kim, T. H.; Acharya, H.; Ito, H.; Kim, H.-C.; Huh, J; Park, C. *Macromolecules* **2008**, *41*, 9290.

(49) Mukherjee, R.; Pangule, R.; Sharma, A.; Tomar, G. *Adv. Funct. Mater.* **2007**, *17*, 2356.

(50) Mukherjee, R.; Sharma, A.; Gonuguntla, M.; Patil, G. K. *J. Nanosci. Nanotechnol.* **2008**, *8*, 3406.

(51) Mukherjee, R.; Sharma, A.; Patil, G. K.; Faruqui, D.; Gooh Pattader, P. S. *Bull. Mater. Sci.* **2008**, *31*, 249.
(52) Mukherjee, R.; Patil, G. K.; Sharma, A. *Ind. Engg. Chem. Res* **2009**, *48*, 8812.
(53) Mukherjee, R.; Sharma, A. *ACS Appl. Mater. Interfaces* **2012**, *4*, 355.
(54) Sharma, A. *Langmuir* **1993**, *9*, 861.
(55) Reiter, G. *Phys. Rev. Lett.* **1992**, *68*, 75.
(56) Xie, R..; Karim, A.; Douglas, J. F.; Han, C. C.; Weiss, R. A. *Phys. Rev. Lett.* **1998**, *81*, 1251.
(57) Mukherjee, R.; Das, S.; Das, A.; Sharma, S. K.; Raychaudhuri, A. K.; Sharma, A. *ACS Nano* **2010**, *4*, 3709.